Analysis of contact less energy transmission system for electronic consumer equipments

Assistant Professor. Dr. Abed Aljabar.F.Ali
Amarah Institute of technology

Abstract:Contactless inductive power transmission system through an air-separation for charging flat shape consumer electronic equipment is presented in this paper. Electromagnetic field plots of the charging arrangement are generated under no-load and loaded conditions so that the distribution of the charging unit could be investigated. Three winding modes of the proposed arrangement have been studied and compared, including complete energization of the winding arrangements. With new results arising from finite element simulation study with ANSYS V.5.4, the theory of the magnetomotive force generation of the multilayer winding array structure could be further understood. The present results provide a base of understanding for future design and optimization of planar contactless charging system.

INTRODUCTION

Bio-implantable devices such as heart pacers, gastric pacer and drug delivery systems require power for carrying out their intended functions. These devices are usually powered through a battery implanted with the system or are wired to an external power source [1]–[4]. Contactless battery chargers have been successfully demonstrated for charging portable consumer electronic equipment such as mobile phones [5]-[7]. This paper presents the investigation of the planar type battery charger by carrying out a finite element simulation field distribution of the planar charging system could also be visualized. With new 2-D and 3-D field plots generated in this finite element simulation study, the theory of planar magnetomotive force generation of the multilayer winding array structure can be further understood. Three working modes, including full-energization mode, selective excitation based on columns and selective energization based on windings are investigated by finite element simulation.

COMPLETE ENERGIZATION MODE

In this mode, the magnetic field distribution of the multilayer winding array is simulated using ANSYS Maxwell-3D finite element software. As shown in figure 1, the charging platform consists of three-layer hexagonal windings which can be connected in series, in parallel or a combination of both. The geometry and number of each winding could be designed flexibly. Limited by the calculating speed of the ANSYS software, a simplified model composed of three-turn windings is used in the simulation as shown in Fig.2. And the values of parameters are also labeled. Each turn is represented by a closed hexagon in the simulation to provide a complete current path. But it must be kept in mind that they are spiral windings in practice. Fig.3 shows the cross- sectional structure of the model. The first working mode of this planar charging is to excite all the windings simultaneously, i.e. full-excitation mode, in order to view the gradual change of MMF (magneto-motive force) distribution.

A. MODE ONE

Only one layer of the winding array structure is energized and simulated with the 3D simulation module. Fig.3 shows the 2D magnetic field distribution superimposed on the x-y plane of the windings. The color and density of the arrows indicates the magnitude of the magnetic field intensity. The instantaneous current in the windings is set as 0.75 A. It can be seen from Fig.3 that the magnitude of the MMF is highest (peak) in the center of the hexagonal winding pattern, and is lowest (valley) at the junction of three windings, as labeled in the figure. It should be noted that each valley is surrounded by 3-peaks and each peak is surrounded by six-valleys.

B. MODE TWO

Another layer is added to the first layer. The MMF peaks of the second layer are placed over the MMF valleys of the first layer. Fig.5 shows the 2D magnetic field distribution superimposed on the X-Y plane of the winding. As expected half of the valleys of the first layar are now filled with MMF peaks by the second layer.

C.MODE THREE

The third simulation is then conducted with three layers of winding arrays. The remaining MMF valleys of the first layer are now filled by the MMF peaks of the third layer. Fig.6 shows the 2D magnetic field distribution superimposed on the x-y plane of the winding and Fig.7 is its 3D angular view. It is important to note that the vertical field in the central region of the charging surface is almost uniform. The field lines curve horizontally at the four edges of the rectangular charging surface. Fig.8 and Fig.9 show the 3-D and 2-D views of the simulated electromagnetic fields in the y-direction respectively. As expected, the electromagnetic fields in the y-direction is fairly uniform especially in the central region. The uniform distribution of the magnetic field over the central region is demonstrated.

MODE THREE WITH A LOAD

A load is placed on the charging surface. Fig.10 shows the field plot of the charging arrangement with a secondary load placed on the top surface. The outer-diameter and inner-diameter of the secondary winding is 40 and 3mm respectively. The number of turns is 18. An opposite current is set in the secondary winding loop in order to simulate the induced load current which brings an opposite flux to cancel the original field, according to Faradays-induction law. It can be seen that the secondary load does slightly distort the magnetic field in the central region. This loading effect is normal.

HIGH FREQUENCY INVERTER CIRCUIT ANALYSIS:

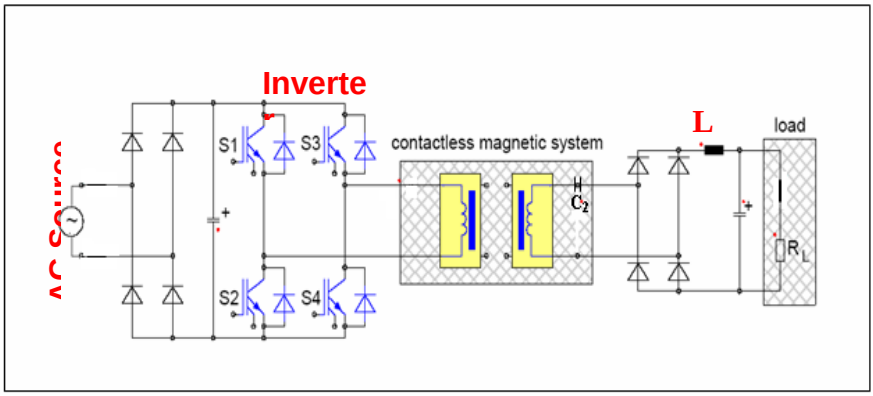

Fig.1: High Frequency Inverter Test Circuit.

Fig.1 shows the schematic of the test circuits, as well as the load in practice**.** The charging platform is excited by an inverter working at high frequency (chosen in the range from 100 to 500 KHZ). Practically, the charging power for portable electronic equipments such as mobile phones ranges from (1.5 to 4 W) and the battery voltage is controlled by the voltage regulator or the battery charging circuit [8] – [9].

Fig.11 to Fig.14 show the secondary voltage distribution in the x-y plane. In these figures the voltage distribution is not exactly the same because of open-loop error. The phenomenon

of central-field sag is observed, regardless of the types and connections of the platforms. The induced secondary voltage drops about a half from the edges to the center, like the simulated results of the vertical magnetic field because the secondary winding can only couple the vertical field, as stated by the induced electromotive force equation of one turn[10]:

$$e = -\frac{d}{dt}\int\int_{s} \mu H.ds$$

Where H is the magnetic field intensity generated by the platform. and S is the area enclosed by the secondary turn. The phenomenon of central-field sag can be explained by the current cancellation effect. At any point in the arrangement where the three layers are fully overlapped [such as point p in Fig.14] there are three equal current vectors that are 120 apart. Each current vectors comes from one of the tree layers, so when all the windings are excited simultaneously without any selection, the planar is similar to a coil which has equivalent turns around the edge of the arrangement.

To verify this explanation, the finite element results of the winding arrays and the equivalent planar coil are obtained and compared in Fig.14. One reason for this phenomenon is illustrated in the figure, the fine line is the original theory in [4]. The resultant MMF over the distance between two adjacent peak positions is equal to 1.0 per unit. But in fact, the valley is practically outside the windings, and so MMF of the valley is not equal to zero, but to a negative value, as illustrated by the bold line. Because there are more windings in the central region of the platform, the absolute value of the negative field in the central region is higher than that in the side part. In addition, the windings along the edges are not fully overlapped and so their MMF distributions are not uniform. The current in the windings and in the planar coil is the same and equal to 0.75 A.

COMPARISON OF THE THREE MODES

In the previous sections**,** the winding current is the same for the tree working modes and the scale in the figures is also the same. Comparison of the results shows that the same current in the windings can generate similar (or slightly higher) magnitude of vertical magnetic field in the effective area of the selectively excited column (or winding) than that in the area near the edges of the fully excited platform, which indicates a similar or slightly higher power transfer ability. But the selective excitation mode can achieve potentially higher efficiency because of much fewer windings excited and thus lower conducting loss. Table 1 compares the approximate normalized magnitude of the vertical magnetic field generated under different operating modes. The average value of [Hz] at the edges of the four columns under full excitation mode is normalized to 1.0. The last column of Table 1, $[\ Hz]^2/n$, is an indicator of efficiency and a higher value is favored [4]. It increases greatly from full excitation mode to selective excitation based on columns.

The value 0f $[\ Hz\ ]^2/N$ when three windings are excited together is not very low, compared to that of other operating modes, because higher magnitude of vertical field is generated. And the uniform distribution of vertical field in its effective area makes mode 3c potentially good choice. Table 1 shows the comparison of three working modes.

Table1: Comparison of Simulated Results for the Three Working Modes.

		Normalized Magnitude of Vertical Field |Hz|	Number of Windings energized	$\frac{\lvert Hz\rvert^2}{N}$
Mode 1 (4 columns)	Edges	1.105	24	0.0428
	Center	0.55	24	0.0105
Equivalent Coil around the Edges	Edges	1.106	6	0.1580
	Center	0.55	6	0.0790
Mode 2 a(1 Column)		1.107	6	0.1667
Mode 2b (2 Columns)		1.107	12	0.0833
Mode 3a (1 Winding Energized)		1.107	1	1.0000
Mode 3b(2 Windings Energized)		1.108	2	0.5000
Mode 3c(3 Windings Energized)		1.348	3	0.5743

APPLICATION OF FERRITE PLATES

The important design issue of the charging arrangement is the insertion of electromagnetic shield on the bottom of the platform. If the electromagnetic field is not shielded in the bottom of the platform, undesirable energy transfer will take place underneath the platform, particularly when the charging platform is placed on a metallic table. To evaluate the shielding effects on the platform using ferrite plates and copper sheets, ferrite plates and then copper sheets are added into the

simulation. Fig.15 shows the cross-sectional structure of the shielded model. The ferrite plates of 0.4mm and copper sheet of 0.07mm are inserted as shown in the figure. Fig.16 shows the magnetic flux distribution in the y-z direction plane. When a no shield is added and b a thin ferrite plate and copper sheet are added. The bottom views of the magnetic field of the charging platform with and without electromagnetic shield are plotted in Fig.17 and Fig.18. Comparison of the simulation shows that the simple shielding structure is effective in this charging platform application.

CONCLUSIONS

A finite element simulation with ANSYS software of a contactless inductive power transfer is presented. Magnetic field plots of the multilayer winding structures are generated and plotted so that the field distribution of the planar arrangement could be better visualized.

The main contribution of this paper is summarized as follows:

1. The complete-energization mode shows "central-field sag" characteristic.
2. The problem of "central-field sag" is explained by current cancellation aspect. By comparing the simulated results, the winding array structure is proved to be equivalent to a concentric planar coil around the edges of the whole area in terms of magnetic field distribution.
3. Two alternative energization modes are proposed and examined both of which can achieve potentially higher efficiency because fewer windings are excited.
4. A simple shielding structure is effective in suppressing the electromagnetic field at the bottom of the structure.
5. The Most important point is, the finite element simulation with ANSYS software which confirms the feasibility and flexibility of the system for efficient power transmission.

REFERENCES

[1] Y. Jang and M.M. Jovanovic, " *A Contactless Electrical Energy Transmission System for*
Portable-Telephone battery Chargers ", IEEE Trans. Ind. Electron, Vol.50, No.3, PP.520-
527, Jun 2003.
[2] S.C.Tang, S.Y.R. Hui and H.S.H. Chung, " *Evaluation of The Shielding Effects on Printed*
Circuit Board Transformers UsingFerrite Plates and Copper Sheets ", IEEE Trans. Power
Electron,Vol.17, No.6, PP.1080-1088, Nov.2002.
[3] C.Fernandz, R.Prieto, O.Garcia and J.Cobos, *" Coreless Magnetic Transformer Design*
Procedure", In Proc. 36th Power Electronics Specialist, Conf. PP. 1548-1554, Jun 2005.
[4] J.T.Strydom and J.D.Van Wyk, *" Electromagneti Modeling For Design and Loss*
Estimation of Resonant Integrated Spiral Planar Power Passives", IEEE Trans. Power
Electron, Vol.19, No.3, PP.603-617, May 2004.
[5] T.C. Neugebauer and D.J. Perreault, " *Filters With Inductance Cancellation Using*
Printed Circuit BoardTransformers", IEEE Trans. Power Electron, Vol.19, No.3, PP.591-
602, May 2004.
[6] C.Kim, D,Seo, J.You,J.Park and B.Cho., *" Design of a Contactless Battery Charger for*
Cellular Phone", IEEE Trans. Ind. Electron, Vol.48, No.6, PP.1238-1247, Dec.2001.
[7] S.Y.R. Hui and W.W.C. Ho, *" A New Generation of Universal Contactless Power*
Transfer System", IEEE Trans. Power Electron, Vol.20, No.3, PP.620-627, May
2005.
[8] X. Liu and S. Y. R. Hui, *" Optimal Design of a Hybrid Winding Structure for Planar*

Contactless Battery Charging Platform", In Proc. IEEE Industry Applications, 41ist Annu.

Meeting, PP.2568-2575, Oct.2006.

[9] " Getting Started : *A Magnetic Force Problem* ", Ansoft Corb, Jun 1997.

[10] " *Material Grade Specification* : 4FI ", In Soft Ferrite Data-Sheets CD-Rom 1998,

Philips Electronics.

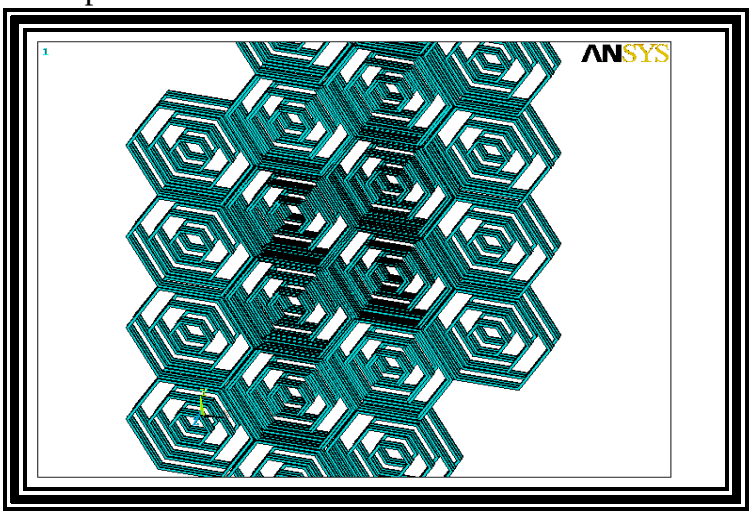

Fig.2: 3-D Model of the Test Arrangement.

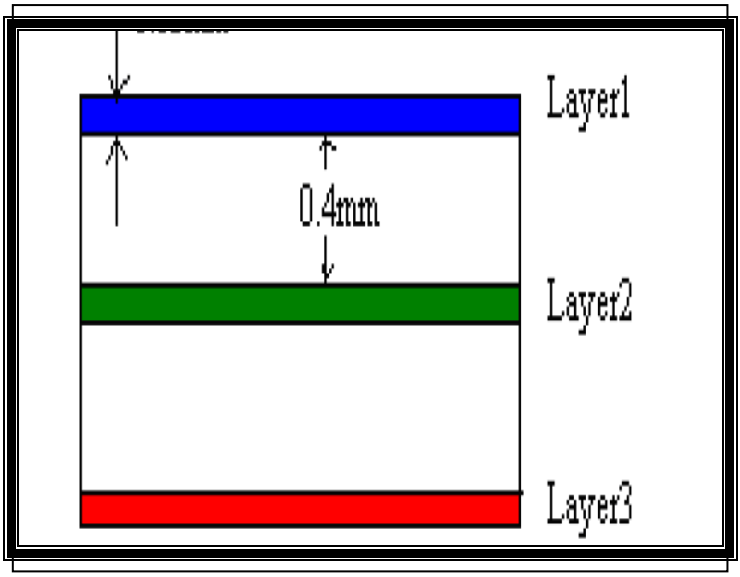

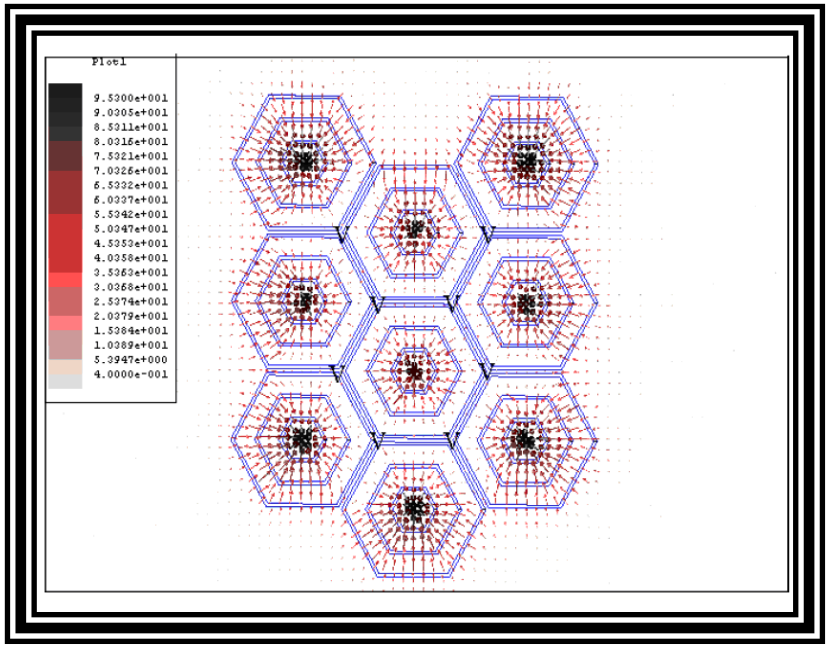

Fig.3: The Cross-sectional Structure of the Test Model.

Fig.4: Simulated Magnetic Flux Distribution of a 1-layer Structure.

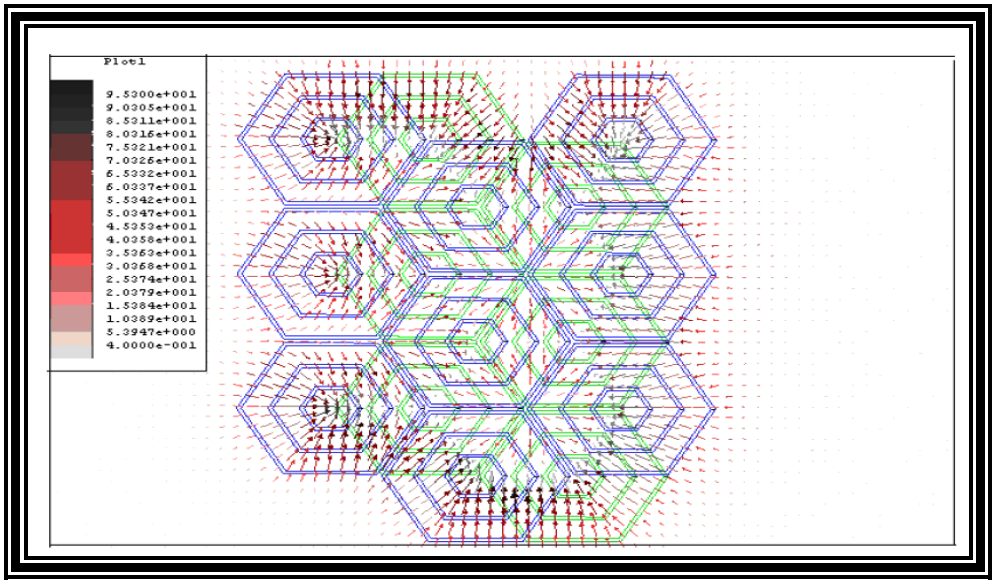

Fig.5: Simulated Magnetic Flux Distribution of a 2-layer Structure.

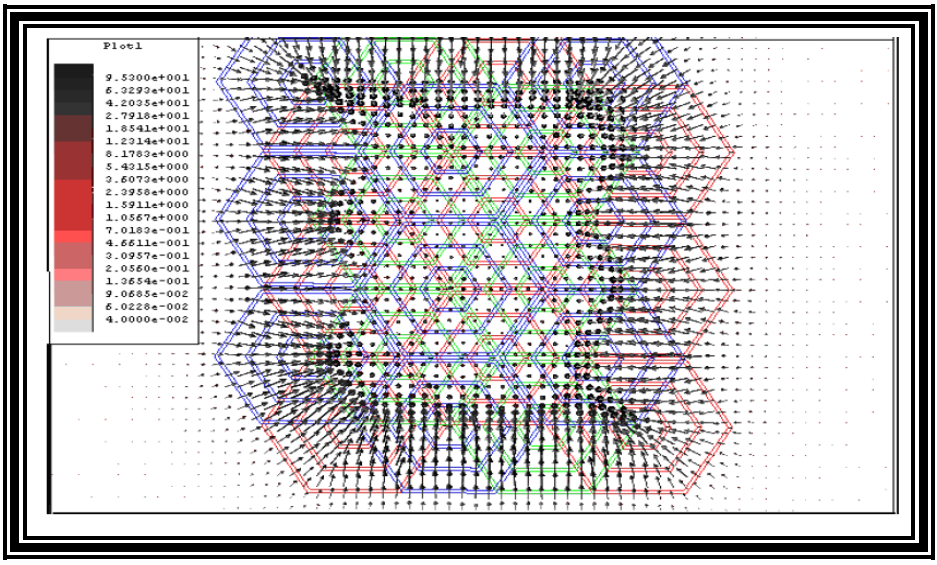

Fig.6: Simulated 2-D Magnetic Flux Distribution of a 3-layer Structure.

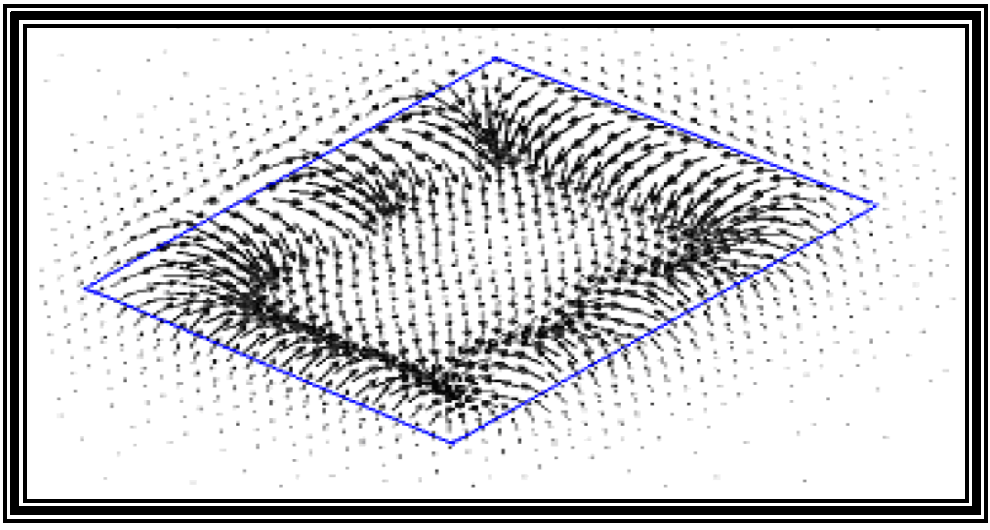

Fig.7: Simulated 3D magnetic flux distribution of a 3-layer structure.

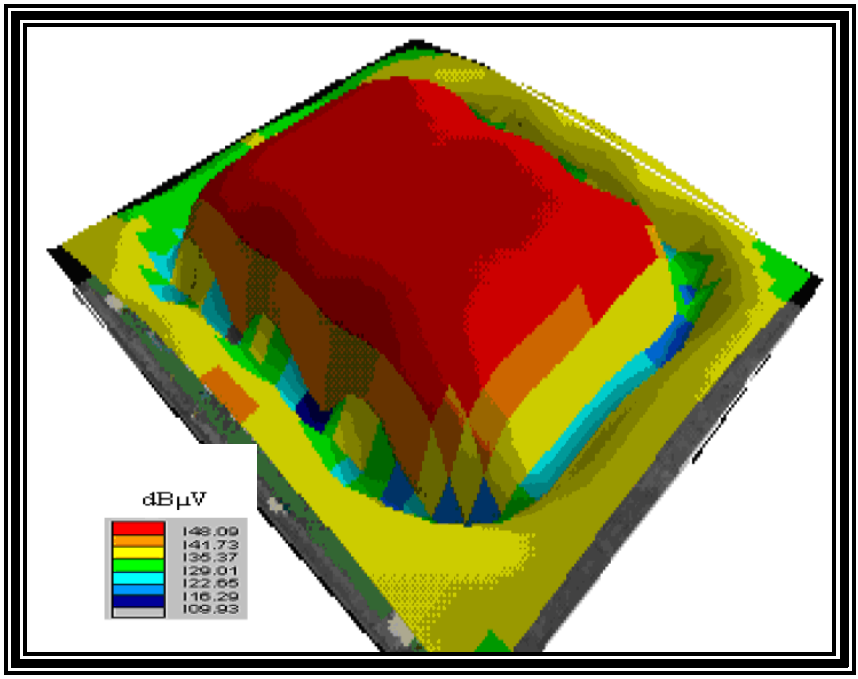

Fig.8: Simulated Electromagnetic Field Distribution in the y-direction , 2-D View.

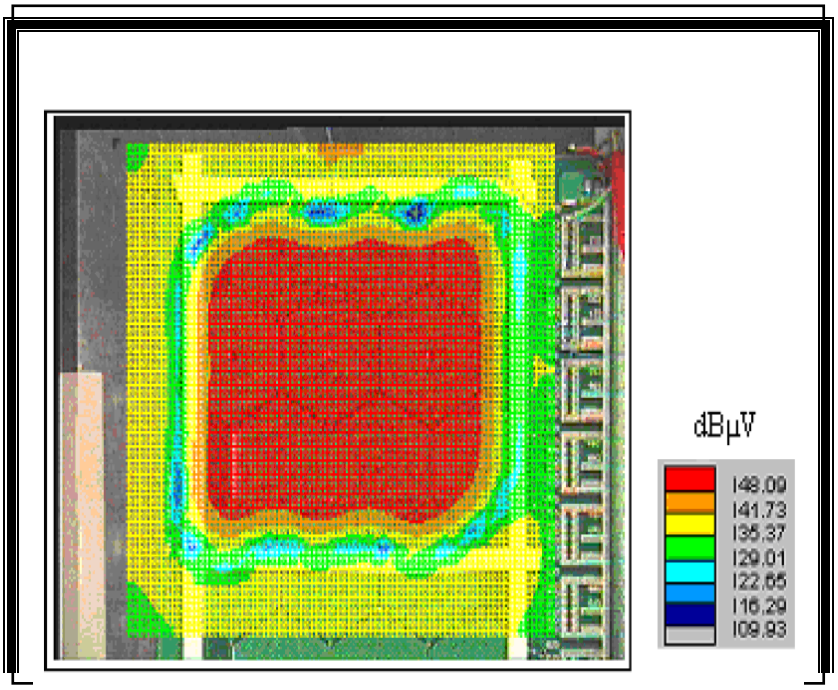

Fig.9: Simulated Electromagnetic Field Distribution in the y-direction , 3-D View.

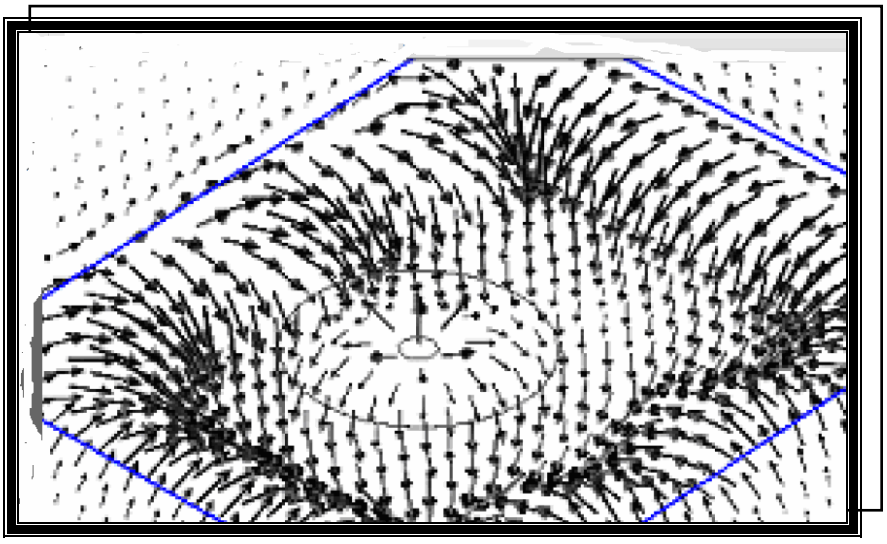

Fig.10: Electromagnetic Field Plot of the Arrangement with Secondary Load.

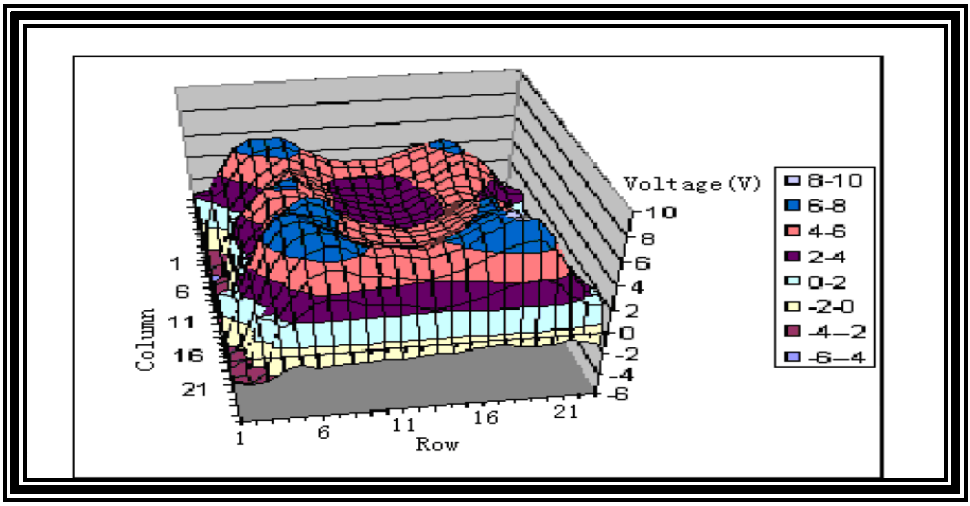

Fig.11: Simulated Results of Secondary Voltage Distribution: Series Connection, f=180 KHZ.

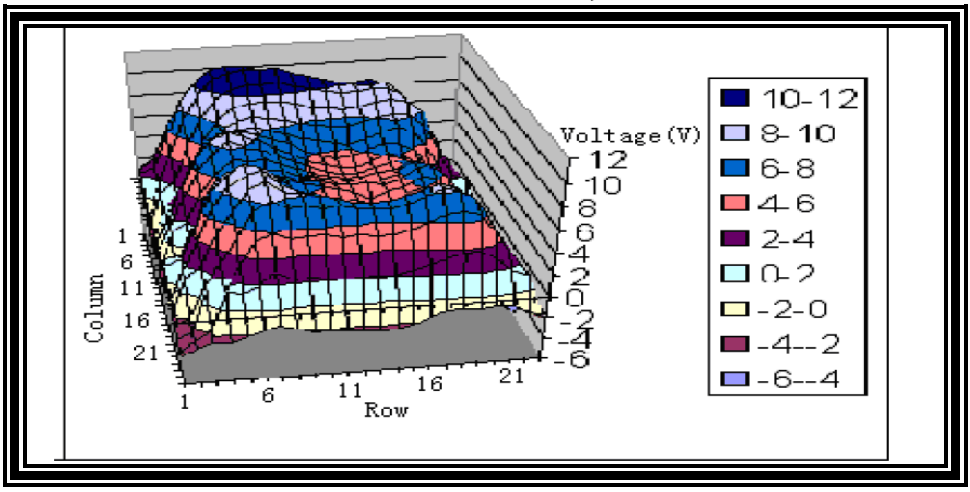

Fig12: Simulated Results of Secondary Voltage Distribution: Series Connection, f=195 KHZ.

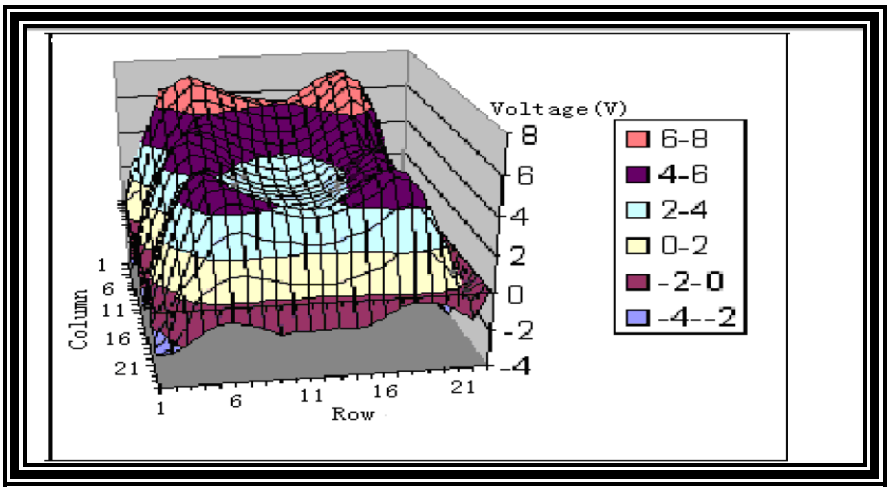

Fig13: Simulated Results of Secondary Voltage Distribution: Series Connection, f=195 KHZ.

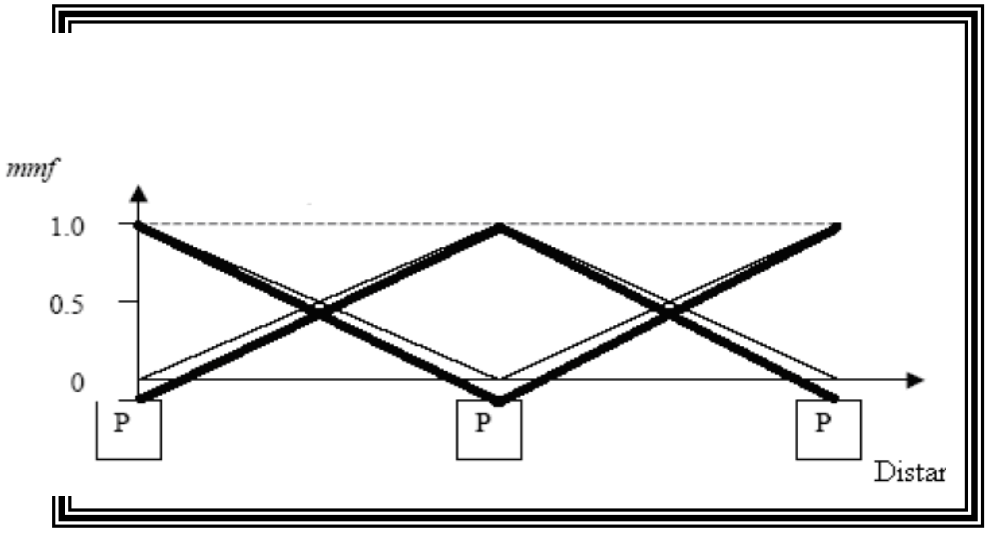

Fig.14: Simulated Electromagnetic Field Distribution Over Distance.

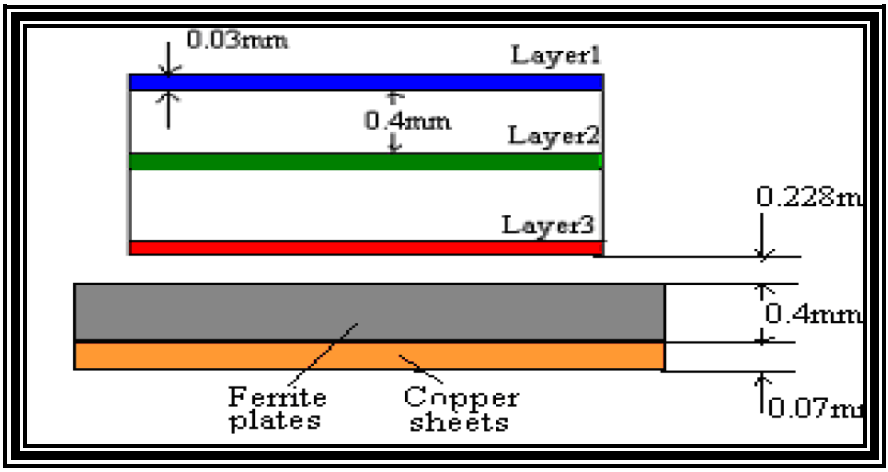

Fig.15.: The Cross-sectional Structure of the Shielded Arrangement.

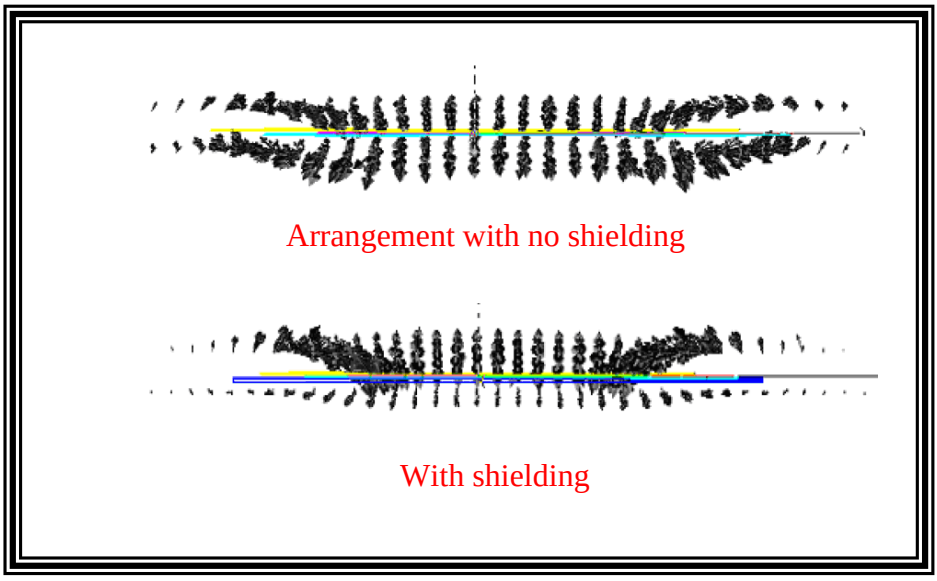

Fig.16: Simulated Electromagnetic Flux Distribution Over Cross-sectional Part.

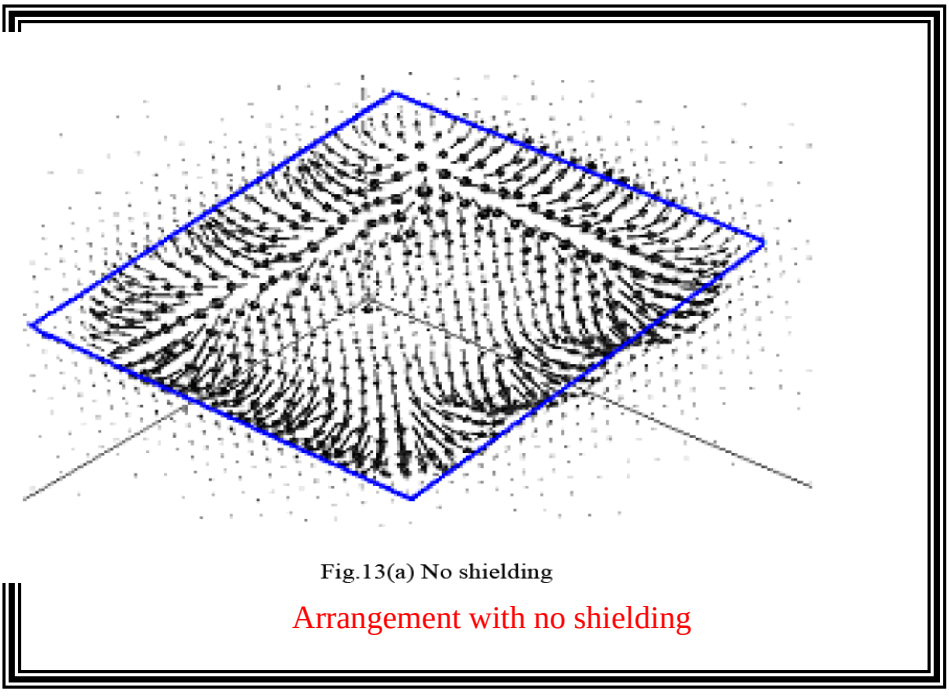

Fig.17: Electromagnetic Field Plots From the Bottom of the Arrangement.

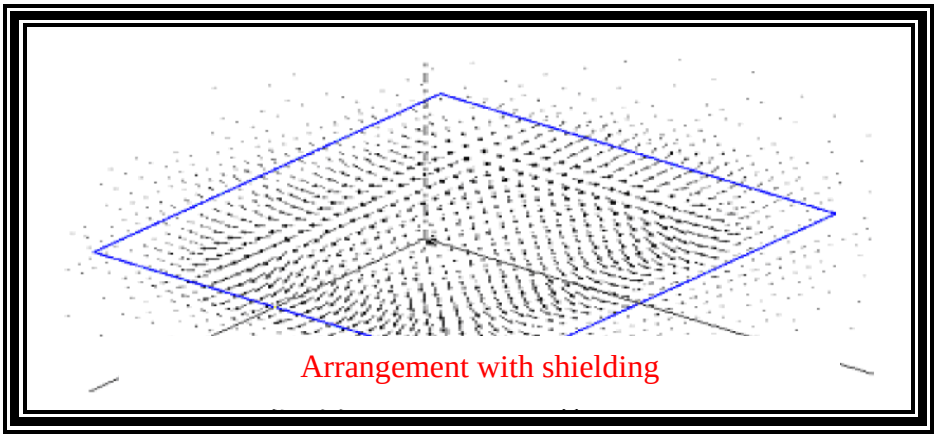

Fig.18: Electromagnetic Field Plots From the Bottom of the Arrangement.

تحليل منظومة نقل الطاقة الكهربائية اللاتلامسية والمستخدمة لتجهيز المعدات الالكترونية

أ.م.د.عبد الجبار فاضل علي
المعهد التقني في العمارة

الخلاصة : يتناول البحث كيفية نقل الطاقة الكهربائية الحثية اللاتلامسية لتجهيز شاحنة معدة الكترونية. استخرجت نتائج المجالات الكهرومغناطيسية للتركيبة المقترحة من عدة طبقات من الملفات بدون و تحت حالة التحميل وذلك لمعرفة وأدراك طبيعة وتصرف انتشار و توزيع هذه المجالات على وحدة الشحن إثناء نقل هذه الطاقة . تم تحليل ومقارنة نتائج ثلاثة أنماط مختلفة لتراكيب الملفات من ضمنها التجهيز الكامل لهذه الملفات و كذلك التجهيز الجزئي. النتائج المستحدثة التي تمت الحصول عليها عن طريق نمذجة و تحليل هذه التقنية باستخدام العناصر المحددة الرياضية مع برنامج (ANSYS) ، وضحت كثيرا من نظرية نقل و انتشار القوى الدافعة الكهربائية المحتثة اللا تلامسية سيما وانه لازالت هذه التقنيات الحديثة قيد البحث. إن هذه النتائج تسهم في إعطاء الأسس المثلى للتصاميم المستقبلية لتقنيات نقل الطاقة الكهربائية اللاتلامسية .